

1 **Electrophysiology reveals that intuitive physics guides visual tracking and working**
2 **memory**

3 Halely Balaban^{1,2}, Kevin A. Smith¹, Joshua B. Tenenbaum¹, Tomer D. Ullman²

4

5 ¹Department of Brain and Cognitive Sciences, Massachusetts Institute of Technology,
6 Cambridge, Massachusetts 02139, USA

7 ²Department of Psychology, Harvard University, Cambridge, Massachusetts 02138, USA

8

9 **Abbreviated title:** Intuitive physics guides visual object tracking

10

11 **Corresponding author:** Halely Balaban (halely@mit.edu)

12

13 **Number of pages:** 37; **Number of figures:** 5;

14 **Number of tables:** 0; **Number of multimedia:** 0; **Number of 3D models:** 0

15 **Number of words for abstract:** 249

16 **Number of words for introduction:** 646

17 **Number of words for discussion:** 1290

18

19 **Conflict of interest:** The authors declare no competing financial interests.

20

21 **Acknowledgments:** This work was supported by the Defense Advanced Research Projects

22 Agency [DARPA] Machine Common Sense program. We thank Roy Luria for his generosity

23 in providing the experimental site.

24 Starting in early infancy, our perception and predictions are rooted in strong expectations
25 about the behavior of everyday objects. These intuitive physics expectations have been
26 demonstrated in numerous behavioral experiments, showing that even pre-verbal infants
27 are surprised when something impossible happens (e.g., when objects magically appear or
28 disappear). Yet, the online mental processes that underlie physical expectations remain
29 hidden. In two EEG experiments (N=32 total, male and female), people watched short
30 videos like those used in behavioral studies with adults and infants, and more recently in AI
31 benchmarks. Objects moved on a stage, and were briefly hidden behind an occluder, with
32 the scene either unfolding as expected, or violating object permanence (adding or
33 removing an object). We measured the contralateral delay activity, an electrophysiological
34 marker of online processing, to examine participants' working memory (WM), as well as
35 their ability to continuously track the objects in the scene. We found that both types of
36 object permanence violation disrupted tracking, even though violations involved
37 perceptually non-salient events (magical vanishing) or new objects that weren't previously
38 tracked (magical creation). The physical violation caused WM to reset, i.e., discard the
39 original scene representation before it could recover and represent the updated number of
40 items. Providing a physical explanation for the violations (a hole behind the occluder)
41 restored object tracking, and we found evidence that WM went on representing the item
42 that disappeared 'down the hole'. Our results show how intuitive physical expectations
43 shape online representations and form the basis of dynamic object tracking.

44 **Significance statement**

45

46 People expect ordinary things to behave in ordinary ways. For example, objects should not
47 appear out of thin air, or suddenly disappear. Decades of research have shown even infants
48 are surprised by physically impossible events. Despite many advances made using
49 behavioral studies, the moment-by-moment neural dynamics of physical expectation
50 violation remain uncharted. Making novel use of electrophysiological markers, we reveal
51 the influence of intuitive physics on online scene processing. Violations of object
52 permanence disrupted object tracking, due to expectations about physical outcomes.
53 Working memory quickly recovered, forming modified scene representations based on
54 physical explanations. This work uncovers a fundamental way in which intuitive physics
55 governs everyday cognition, and provides a new neural method for studying central
56 cognitive processes.

57 **Introduction**

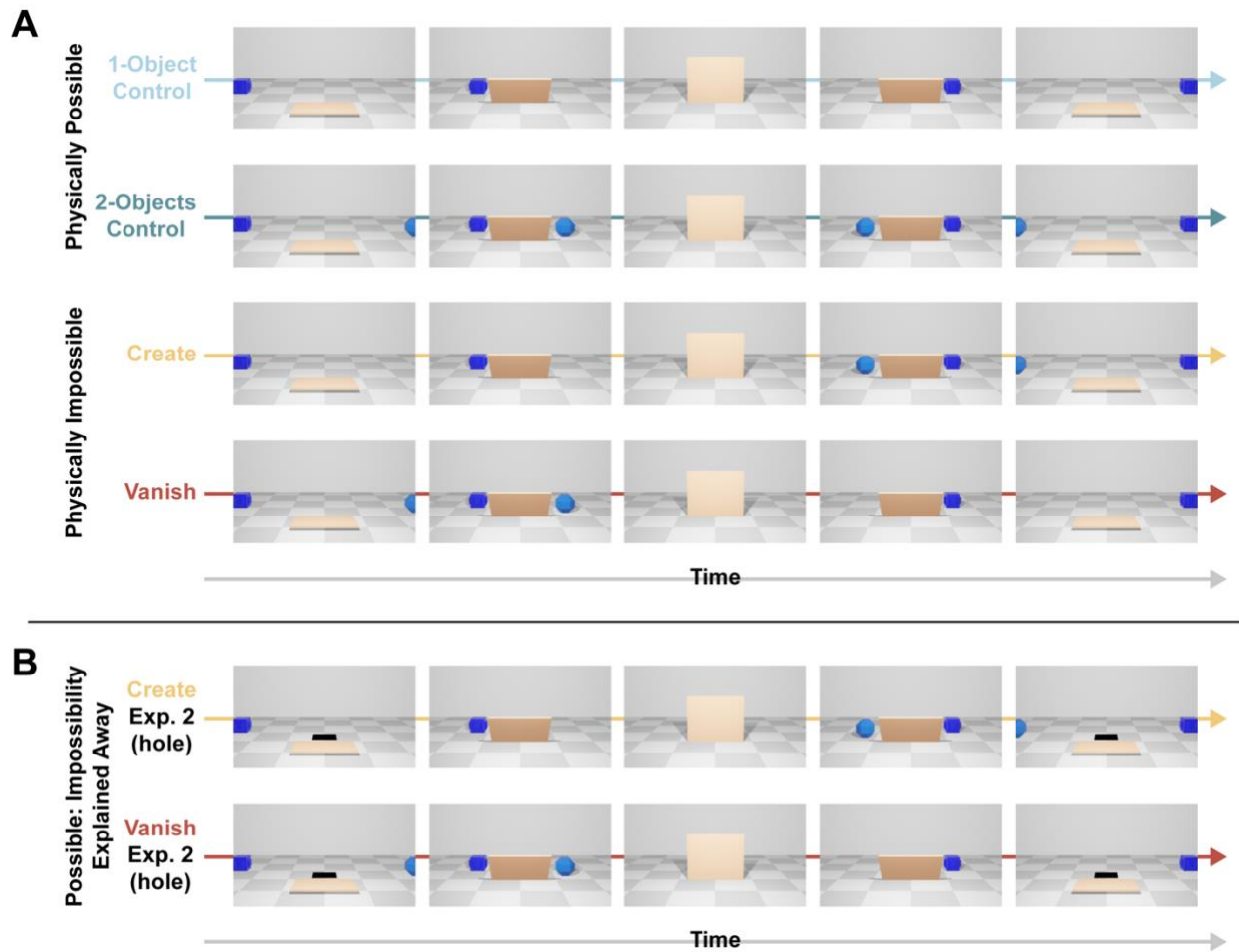
58

59 People have basic expectations about the physical behavior of everyday objects. Objects do
60 not simply disappear and reappear, and solid bodies do not pass through one another or
61 break apart for no reason. Such expectations, known as ‘intuitive physics’, help us to
62 efficiently perceive, predict, and interact with the world around us (Spelke, 1990; Battaglia
63 et al., 2013; Kubricht et al., 2017). Core physical expectations are present in very early
64 infancy, and shared by many non-human animals (Baillargeon et al., 1985; Wynn, 1992; Xu
65 and Carey, 1996; Cacchione and Krist, 2004). The existence of these expectations has been
66 established over decades, mostly through measures of overt surprise in the face of
67 physically impossible events. More recent studies have used computational and
68 neuroscientific methods to provide insight into the cognitive mechanisms and brain
69 regions involved in intuitive physics (Fischer et al., 2016; Bear et al., 2021; Piloto et al.,
70 2022). Yet despite the fundamental role of intuitive physics in our understanding of the
71 world, its moment-by-moment neural processing remains largely unknown. In this paper,
72 we use EEG methods and behavioral displays to study the unfolding neural dynamics of
73 physical expectations, from representation, to the detection of anomalies, to resolution.

74 To uncover the ongoing processing of intuitive physics, we adopted a novel
75 approach of targeting working memory (WM). This mental workspace holds information in
76 an active state, ready to be accessed and manipulated (Baddeley, 1992; Luck and Vogel,
77 1997). WM is involved in both classic memory paradigms, and whenever material has to be
78 held online (Blaser et al., 2000; Carlisle et al., 2011; Tsubomi et al., 2013). We modified a
79 standard WM paradigm, to include stimuli based on classic developmental studies (Wynn,

80 1992) and recent AI-benchmarks that probe physical expectations in machines (Piloto et
81 al., 2022).

82 In two experiments, people watched short animations of one or two objects crossing
83 a stage (Figure 1; example videos: https://youtu.be/w_jalxFD0HU). The scenes either
84 unfolded as expected, or contradicted object permanence by having an object appear or
85 disappear. Using EEG, we recorded scalp electrical activity as people watched the
86 animations, and tested, for the first time, how violations of physical expectations are
87 processed online.



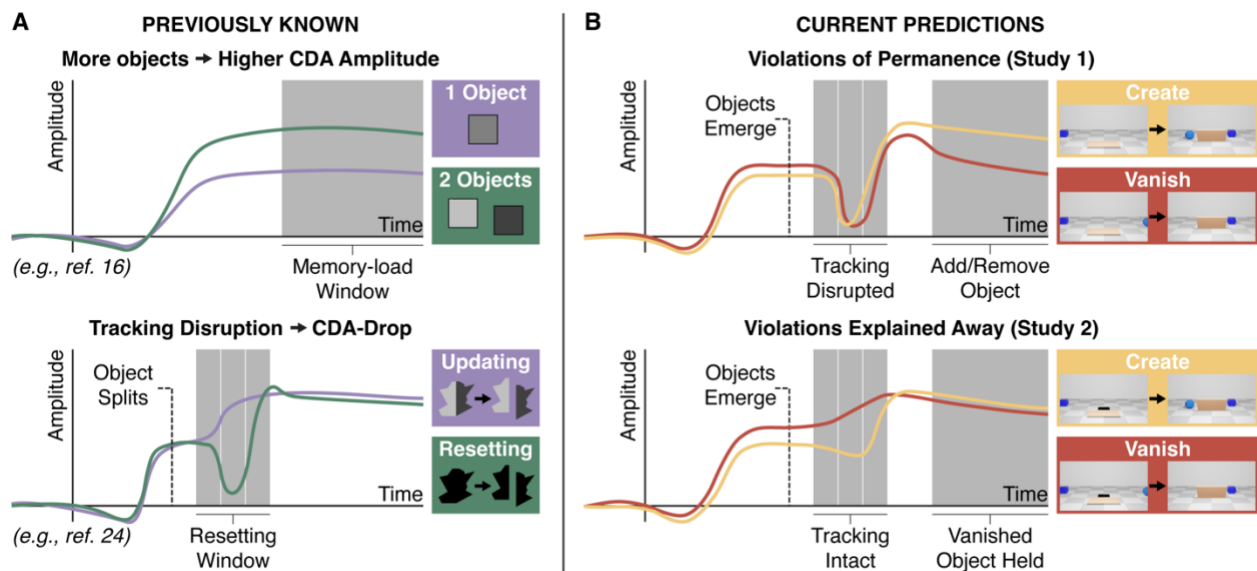
88

89 **Figure 1.** Frames from the animations used as stimuli. (A) Experiment 1's conditions. Top
 90 to bottom: 1-Object and 2-Objects Controls, Create, and Vanish. Note that Create starts like
 91 1-Object and ends like 2-Objects, while Vanish is the opposite. (B) Experiment 2's Create
 92 and Vanish condition.

93

94 To evaluate moment-by-moment active processing, we isolated contralateral delay
 95 activity (CDA; see Vogel and Machizawa, 2004; Vogel et al., 2005; Luria et al., 2016), an
 96 event-related potential (ERP) index of WM. The CDA's amplitude reflects representational
 97 load (while being immune to related factors, for a review see Luria et al., 2016), rising
 98 when more items are held online (Figure 2A, top). The CDA also reflects the dynamics of

99 the pointer system, an indexing process connecting online representations with perception.
 100 The pointer system implements a one-to-one correspondence through which a specific
 101 representation in WM can be accessed and updated when the analogous real-world item
 102 changes (Kahneman et al., 1992; Scholl and Pylyshyn, 1999; Pylyshyn, 2000; Balaban and
 103 Luria, 2017). If the WM-perception correspondence is disrupted (e.g., if an object splits in
 104 two), WM resets (Balaban and Luria, 2017; Balaban et al., 2018a, 2018b, 2019a). Resetting
 105 is accompanied by a reliable transient drop in CDA amplitude (Figure 2A, bottom),
 106 indicating that an event interrupted the pointer system's tracking ability. The CDA-drop
 107 specifically taps into pointer system disruption, and does not reflect related but distinct
 108 factors such as general surprise (Balaban and Luria, 2019; see also the Discussion).
 109



110
 111 **Figure 2.** Schematic of past results and current predictions. (A) Previous CDA-based
 112 findings regarding online representations (top) and tracking (bottom). (B) Current
 113 predictions in Experiment 1 (top) and 2 (bottom).

114 The excellent temporal resolution of ERPs allowed us to examine different pre-
115 defined time-windows of the CDA amplitude, to uncover evolving mental processing in a
116 fine-grained manner (Figure 2B). Specifically, we tested whether violations of object
117 permanence (Experiment 1) interrupt object tracking, causing a CDA-drop in the
118 previously-established resetting window, followed by the appropriate removal or addition
119 of an object from WM. We also hypothesized that if violations are explained away
120 (Experiment 2), the modified expectations about physical dynamics may prevent
121 disruption, leading to no resetting, and no removal of the vanished object from WM.

122

123

124

125 **Materials and Methods**

126

127 Data, code, and video examples are available at the Open Science Framework:

128 <https://osf.io/csarg>.

129

130 **Participants**

131 Participants were students with normal or corrected-to-normal visual acuity and normal
132 color-vision, who gave informed consent following the procedures of a protocol approved
133 by the Massachusetts Institute of Technology Committee on the Use of Humans as
134 Experimental Subjects under protocol 1912000059. Due to the COVID-19 global pandemic,
135 the experiments were run at Tel Aviv University, Israel. Participants were notified of their

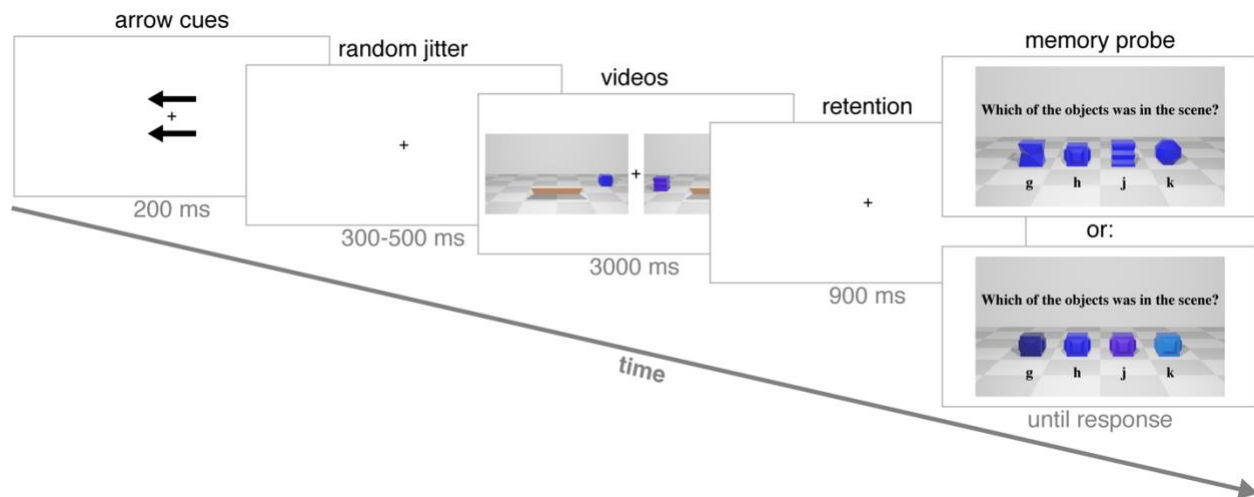
136 rights before the experiment, were free to terminate participation at any time, and were
137 compensated monetarily for their time at a rate of \$30 an hour.

138 Each experiment included 16 naïve participants (11 females, mean age 24 in
139 Experiment 1, and 14 females, mean age 24 in Experiment 2). Sample size was determined
140 based on the smallest effect size in the study with the most similar analysis method
141 (Balaban and Luria, 2017), which was $d = 0.8$, entailing 16 participants for 80% power.
142 Because the experiment required holding fixation and avoiding blinks for a relatively long
143 time (roughly 6 seconds on each trial), participants who could not perform the task under
144 these limitations were released after the first few blocks and replaced (3 in each
145 experiment). Another participant in Experiment 1 was released and replaced for failing to
146 understand the task, and another one was released due to electrode malfunction.

147

148 **Stimuli and Procedure**

149 In this study, we presented videos that may or may not contain a physical violation, and we
150 measured EEG to examine how the scenes are represented. As is standard, this requires
151 showing two videos – one for each hemisphere – and pre-cuing which side to pay attention
152 to. Using this lateralized display allows defining the contralateral and ipsilateral
153 hemispheres, and subtracting them to get rid of any common perceptual factors. To ensure
154 participants pay attention to the videos and hold objects in WM, after the animations'
155 presentation they were given a task, to pick out one of the objects that they had seen from a
156 set of objects. Figure 3 presents the trial sequence.



157
 158 **Figure 3.** Example of a trial sequence in Experiments 1 and 2. Black arrows indicated to
 159 participants which side is relevant for the upcoming trial. The video animations included
 160 objects crossing the floor, as an occluder went up and down, briefly hiding them from view.
 161 Objects' movement and the occluder were irrelevant to the task. After a retention interval,
 162 subjects selected the previously presented object from 4 options, which were either all the
 163 same color and varying in shape (a shape test; top), or all the same shape and varying in
 164 color (a color test; bottom).

165
 166 Each trial started with a 1,000 ms display of a fixation black cross $0.7^\circ \times 0.7^\circ$ of
 167 visual angle from a viewing distance of approximately 60 cm) in the center of a grey screen
 168 (RGB values: 180, 180, 180). Then, two black arrows ($3^\circ \times 1^\circ$) appeared above and below
 169 fixation for 200 ms. The arrows pointed either left or right randomly (with an equal
 170 probability), and this indicated the side to which participants were asked to attend for the
 171 upcoming trial. After another 300-500 ms (randomly jittered) fixation display, a video
 172 animation was played on each side of the fixation. Each video spanned about 21° in width
 173 and 12° in height, and was placed at a distance of 4.2° from the fixation, and at the middle

174 of the screen's height. The videos on both sides were always from the same condition (see
175 below; from here on, when describing the number of items, we always refer to the relevant
176 side), with all other details drawn randomly (without replacement) independently between
177 the sides. On the main trials, the videos played for 3 second. On catch trials, the videos
178 played for only 300 ms. The goal of these short trials was to ensure participants paid
179 attention not only to the end of the animation. They made up 25% of the trials in the first
180 block, and 10% in all other blocks. Catch trials were not analyzed. After the video
181 animations, a 900 ms retention interval was presented, with only the fixation visible on
182 screen. Then a memory probe appeared, including an image of 4 objects, from which
183 participants chose the one that appeared in the video they saw on the relevant side of the
184 screen. Responses were made via button press (using the "g", "h", "j", and "k" keys on a
185 standard keyboard, based on the objects' location in the image, from left to right).
186 Responses were unspeeded and no feedback was provided. Participants were asked to hold
187 fixation throughout the trial, and to blink only when they press the response key.
188 Participants completed 15 practice trials, followed by 16 experimental blocks of 50 trials
189 each, for a total of 800 trials (including catch trials), and about 180 trials per condition. The
190 experimental session took 2.5-3 hours (including EEG preparation).

191 Animations were created in Blender, and rendered in the Eavee engine at 24 frames
192 per second. Videos displayed a light-grey and white checkerboard pattern floor, a white
193 back wall, and a rectangular light-orange screen, referred to as the occluder, in the middle
194 of the scene. The occluder started off on the floor, went up until it stood vertically midway
195 through the video, and lowered back down. Additionally, each video included one or two
196 objects crossing the floor from one side to the other, with the occluder hiding them from

197 view for 625 ms. When the animation included two objects, they moved in opposite
198 directions, and one of them was slightly closer to the occluder than the other, so that they
199 would not collide.

200 There were 4 possible un-namable shapes, and 4 possible colors that were all
201 shades of blue (the exact rendered color changed across the object's surface because of the
202 irregular shapes' shading; RGB values are reported based on one representative area: 45,
203 45, 142; 60, 60, 230; 105, 60, 220; 45, 130, 210), for a total of 16 possible objects. Each
204 object's movement direction (from right to left or from left to right), color, and shape were
205 determined randomly without replacement in each trial.

206 There were 4 conditions, varying in the number of objects at the beginning and end
207 of the animation (see Figure 1A). In the two physically possible Control conditions, either
208 one or two objects simply passed behind the occluder (the 1-Object and 2-Objects Controls,
209 respectively). There were two physically impossible conditions: Create, where one object
210 went behind the occluder but two exited, and Vanish, where two objects went behind the
211 occluder but only one exited. Thus, in the Create condition the video's first half was
212 identical to the 1-Object Control and its second half was identical to the 2-Objects Control,
213 and vice versa for the Vanish condition. The Create and Vanish conditions constitute
214 violations of object permanence, which translates to a change in the number of objects,
215 allowing us to leverage the CDA's set-size sensitivity (see below). In the Vanish condition,
216 the item that disappeared was never probed, though participants were not explicitly told of
217 that.

218 There were only two differences between Experiments 1 and 2. First, in the Create
219 and Vanish conditions of Experiment 2, a small black rectangle was placed right behind the

220 occluder throughout the trial (see Figure 1B). Importantly, this black area was only visible
221 when the occluder was down (i.e., at the beginning and end of the trial). The second
222 difference compared to Experiment 1 was the explanation provided to participants before
223 the experiment started. Participants in Experiment 2 were told that the black area is a hole
224 in the floor, meaning that if the trial starts with two objects, one is going to fall down (the
225 front object), and if the trial starts with one object, one is going to “climb up” from the hole,
226 using a hidden leverage. Participants were also shown example video of the different
227 conditions, and a demonstration of what the Vanish condition would look like if the
228 occluder wasn’t there (showing an object falling down the “hole”).

229

230 **EEG Recording and Analysis**

231 EEG was recorded inside a shielded Faraday cage, using a BioSemi ActiveTwo system, from
232 32 scalp electrodes placed at a subset of the extended 10-20 system’s locations, and from
233 two electrodes placed on the mastoids, which served as reference. EOG was recorded from
234 two electrodes placed 1 cm from the external canthi, and from an electrode placed 2 cm
235 beneath the left eye. Data was digitized at 256 Hz.

236 Offline signal processing was performed using the EEGLAB (Delorme and Makeig,
237 2004) and ERPLAB (Lopez-Calderon and Luck, 2014) toolboxes, and custom Matlab (The
238 Mathworks, Inc.) scripts. All electrodes were referenced to the average of the left and right
239 mastoid electrodes. Continuous data was segmented into epochs from -200 to +3900 ms
240 from animations’ onset (corresponding to the end of the retention interval). Artifact
241 detection was performed on the EOG electrodes using a sliding window peak-to-peak
242 analysis, with a threshold of 80 μ V. This procedure resulted in a mean rejection rate of

243 9.2% in Experiment 1, and 9.5% in Experiment 2 (for evidence that eye movements are not
244 responsible for the CDA or the resetting-drop, see Kang and Woodman, 2014; Balaban and
245 Luria, 2017, 2019; Balaban et al., 2018a). For plotting purposes, the epoched data were
246 low-pass filtered using a noncausal Butterworth filter (12 dB/oct) with a half-amplitude
247 cutoff point at 30 Hz. Statistical analysis was performed on the unfiltered data, to avoid
248 potential effects of filtering on the results.

249 Epoched data were averaged separately for each condition, and difference waves
250 were calculated by subtracting ipsilateral from contralateral activity, relative to the
251 memorized side on each trial. As was done in previous research (e.g., Balaban and Luria,
252 2017; Balaban et al., 2018a, 2019a), we focus on the results from the average of 3 parietal-
253 occipital electrode pairs – P7/8, Po3/4, and Po7/8 – but similar patterns of activity were
254 found in each pair separately.

255

256 **Experimental Design and Statistical Analyses**

257 In order to examine the maintenance and tracking of online representations in WM during
258 a physics-violation task, we isolated the CDA (Vogel and Machizawa, 2004; Vogel et al.,
259 2005; Luria et al., 2016). The CDA is an ERP component reflecting online processing in
260 visual WM. It was first reported in memory tasks, but can be measured equally well when
261 items are held in WM while being completely visible (Tsubomi et al., 2013), like in search
262 or tracking tasks (Drew and Vogel, 2008; Luria and Vogel, 2011b). Numerous studies have
263 shown that CDA amplitude is not sensitive to processes that are related to, but distinct
264 from, WM, such as spatial attention or task difficulty (Vogel and Machizawa, 2004;
265 McCollough et al., 2007; Ikkai et al., 2010; Feldmann-Wüstefeld et al., 2018, and, for a

266 review, see Luria et al., 2016). Similarly, the resetting-drop in CDA amplitude is extremely
267 specific: When the mapping between WM representations and perceptual input is
268 disrupted there is a characteristic drop, whereas extremely similar situations (even within
269 experiment and participants) that allow this mapping to hold lead to a smooth change in
270 amplitude (Balaban and Luria, 2017; Balaban et al., 2018a, 2019a, and, for a review, see
271 Balaban and Luria, 2019). Last though crucial, the CDA-drop does *not* reflect general
272 surprise. Rather, it is the result of a specific disruption to object tracking. The effect persists
273 after many dozens of exposures to the disrupting events, and can also be observed for
274 events that are completely predictable (Balaban et al., 2019b).

275 Based on prior work, we analyzed the CDA in several pre-defined time-windows (for
276 a similar approach in different contexts, see Luria and Vogel, 2011a; Drew et al., 2012,
277 2013; Balaban and Luria, 2015; Peterson et al., 2015; Balaban and Luria, 2016a, 2016b).
278 First, to examine tracking, for each condition we compared mean amplitude across two
279 previously-defined time-windows (Balaban and Luria, 2017): the resetting window, 200-
280 300 ms after the critical event, and the pre-resetting baseline window, immediately
281 preceding it, i.e., 100-200 ms after the critical event. Here, the critical event was the
282 moment when items started to emerge from behind the occluder, or, in the Vanish
283 condition, the time in which an item should have emerge but didn't. This happened 1896
284 ms after the onset of the video.

285 We additionally examined the window immediately following the resetting window
286 (300-400 ms after the critical event). In previous studies involving object separation, this
287 delay was enough time for the resetting process to finish (e.g., Balaban and Luria, 2017).

288 We compared this time-window to the pre-resetting baseline time-window, to test whether
289 in our study WM recovers as quickly as in other contexts.

290 To establish scene reinterpretation, we compared mean amplitude during the
291 retention interval (3200-3900 ms after trial onset; note that the CDA takes about 200 ms to
292 respond, e.g., to initially rise, see Vogel et al., 2005) across the different conditions.
293 Specifically, we examined whether, after the video ended, participants represented the
294 Create and Vanish conditions similarly to 1 object or to 2 objects (i.e., whether the
295 amplitude in each impossible condition is lower than that of the 2-Objects Control, or
296 higher than that of 1-Object Control).

297 A resetting-drop was established via a within-subjects Analysis of Variance
298 (ANOVA), with Time (pre-resetting baseline vs. resetting, and pre-resetting vs. prolonged
299 resetting) and Condition as independent factors on mean amplitude as the dependent
300 measure. The final representation was examined with a within-subjects ANOVA, with
301 Condition as an independent factor, on mean amplitude during the retention time-window
302 as the dependent measure. Finally, we analyzed behavioral performance in the task with a
303 one-way within-subjects ANOVA with condition as an independent factor on accuracy as a
304 dependent measure. We followed these ANOVAs with planned comparisons (contrasts), the
305 results of which we focus on, for simplicity. We additionally report effect sizes for all
306 statistical comparisons, and 95% confidence intervals (CIs) for the difference between
307 conditions.

308 **Results**

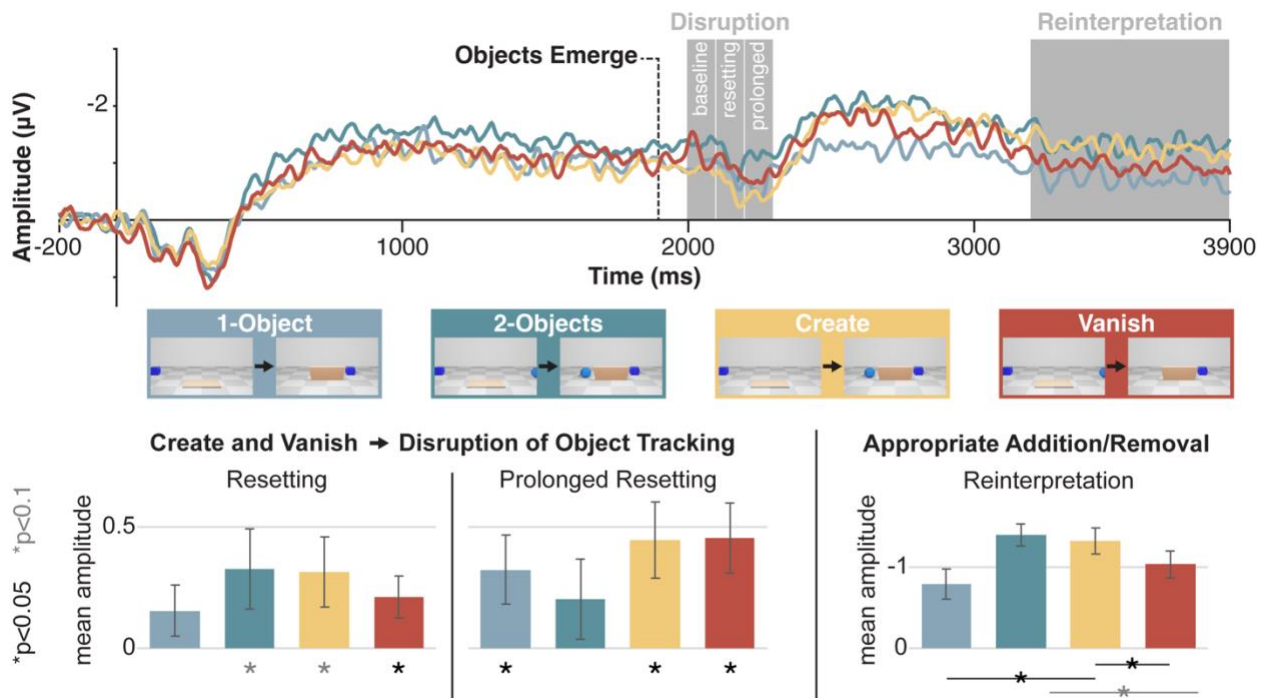
309

310 **Experiment 1: Active representations rely on intuitive physics**

311 In Experiment 1, we tested how object permanence violations affect online maintenance
312 and tracking. Within a WM task, participants ($n = 16$) watched animations of objects
313 moving across a stage, behind a rising screen, and back out as the screen lowers (Figure
314 1A). In the Control conditions, the animations proceeded as expected. In the impossible
315 conditions, while the screen was up an object was added (Create) or removed (Vanish),
316 seeming to appear or disappear magically. It is in principle possible that object tracking is
317 sensitive only to low-level visual properties, rather than physical expectations. In this case,
318 the CDA should rise or fall smoothly. However, if events that contradict intuitive physics
319 disrupt the ongoing function of the pointer system, both Create and Vanish should trigger a
320 CDA-drop (resetting).

321 To test the possible disruption of the pointer system, we compared the CDA
322 amplitude in the resetting time-window (200-300 ms after the critical event, when an item
323 appeared or failed to appear) to the baseline time-window which immediately precedes
324 any potential CDA-drop (Balaban and Luria, 2017). We also compared the baseline to the
325 immediately subsequent time-window (300-400 ms after the critical event). After
326 establishing a significant interaction of Time and Condition ($F(3,45) = 3.31, p = 0.028$), we
327 focused our analysis on the violation conditions. We found a CDA-drop for both types of
328 object permanence violation (Create and Vanish), with lower amplitude in the resetting
329 time-window (Figure 4). This effect was marginally significant in the Create condition
330 ($F(1,15) = 4.47, p = 0.05, d = 0.5, 95\% CI = [0.0, 0.63] \mu V$), and significant in the Vanish

331 condition ($F(1,15) = 5.61, p = 0.03, d = 0.6, 95\% \text{ CI} = [0.02, 0.4]$). As detailed above, this
 332 CDA-drop does *not* reflect a general surprise from some event, but specifically marks a
 333 disruption to the ongoing function of the pointer system. So, the results demonstrate that
 334 the pointer system depends on intuitive physics for object tracking.
 335
 336



337
 338 **Figure 4.** EEG results for Experiment 1. Top: CDA waveforms by condition. Dashed line
 339 indicates when objects emerge behind the lowering screen. Analyzed time-windows are in
 340 grey. Bottom: Mean amplitude by condition and time-window; error bars show standard
 341 error. From left to right: Resetting minus baseline (indicating object tracking disruption),
 342 immediately following window minus baseline (indicating prolonged object tracking
 343 disruption), and retention interval amplitude (indicating scene reinterpretation, i.e., the
 344 number of represented objects at the end of the trial). Asterisks show significant (black)

345 and marginally significant (grey) contrasts, following the ANOVAs (see Materials and
346 Methods).

347
348 Resetting even persisted in the following time-window, with significantly lower
349 amplitudes (as compared with the pre-resetting window) for both the Create ($F(1,15) =$
350 $7.67, p = 0.01, d = 0.7, 95\% CI = [0.1, 0.79]$) and Vanish ($F(1,15) = 9.08, p = 0.01, d = 0.8,$
351 $95\% CI = [0.13, 0.78]$) conditions. Though we cannot directly compare the current results
352 with experiments that use different stimuli, the prolonged resetting effect suggests that the
353 pointer system took longer to recover from violations of object permanence than what was
354 previously reported for 2D events like separation, in which the same delay was enough for
355 the system to recover (e.g., Balaban et al., 2019a).

356 In addition to the predicted resetting effects in the violation conditions, we found
357 possible marginal evidence for shorter-lived resetting effects in the Control conditions. In
358 the resetting time-window, there was borderline evidence for a drop in the 2-Objects
359 Control ($F(1, 15) = 3.66, p = 0.08, d = 0.5, 95\% CI = [-0.04, 0.69]$), and no evidence for this
360 effect in the 1-Object Control ($F(1, 15) = 1.97, p = 0.18, d = 0.4, 95\% CI = [-0.08, 0.39]$). In
361 the later time-window, there was no evidence for resetting in the 2-Objects Control ($F(1,$
362 $15) = 1.38, p = 0.26, d = 0.3, 95\% CI = [-0.17, 0.57]$), and there was an effect for the 1-Object
363 Control ($F(1, 15) = 4.88, p = 0.04, d = 0.6, 95\% CI = [-0.01, 0.64]$). We believe these effects, if
364 they can be considered that, are artifacts. Beyond the fact that the evidence for them was
365 not strong in this experiment, the results of Experiment 2 (see below) show that a direct
366 replication of the Control conditions result in no effect at all. Still, if one were to try to
367 account for these possible effects, we would suggest that the violations of intuitive physics

368 in the impossible conditions may have led participants to undergo a resetting process in *all*
369 conditions, though more weakly in the Control conditions. In support for this possibility, it
370 has recently been shown that when pointer-disruption events become prevalent, a
371 resetting process will occur in situations that do allow the mapping to hold (Friedman and
372 Luria, 2022).

373 In addition to tracking disruption, we compared the final CDA amplitude (during the
374 retention interval) of the different conditions, to test how WM representations changed as
375 the scene evolved. We found a significant effect of Condition ($F(3,45) = 4.46, p = 0.008$). We
376 expected that by the end of the trial, the CDA amplitude would reflect the updated number
377 of items in the scene. In line with this, a comparison of the different conditions indicated
378 that the CDA amplitude was consistent with an item being added in the Create condition,
379 and removed in the Vanish condition. The CDA amplitude in Create was higher than the 1-
380 Object Control ($F(1,15) = 9.77, p = 0.01, d = 0.8, 95\% CI = [0.17, 0.9]$), and similar to the 2-
381 Objects Control ($F < 1, p = 0.76, d = 0.1, 95\% CI = [-0.41, 0.55]$). The CDA amplitude in the
382 Vanish condition was significantly lower than Create ($F(1,15) = 6.36, p = 0.02, d = 0.6, 95\%$
383 $CI = [0.05, 0.58]$), marginally lower than the 2-Objects Control ($F(1,15) = 3.94, p = 0.07, d =$
384 $0.5, 95\% CI = [-0.03, 0.8]$), and similar to the 1-Object Control ($F(1,15) = 1.81, p = 0.2, d =$
385 $0.3, 95\% CI = [-0.13, 0.57]$). These findings indicate that participants successfully and
386 rapidly adjusted their representations after object permanence violations, adequately
387 adding or removing objects from WM.

388 For completeness, we also examined behavioral performance, and found a
389 significant effect of Condition on accuracy ($F(3,45) = 41.69, p < 0.001$). We stress that
390 accuracy in our task does not tap into the ongoing dynamics of representations in WM,

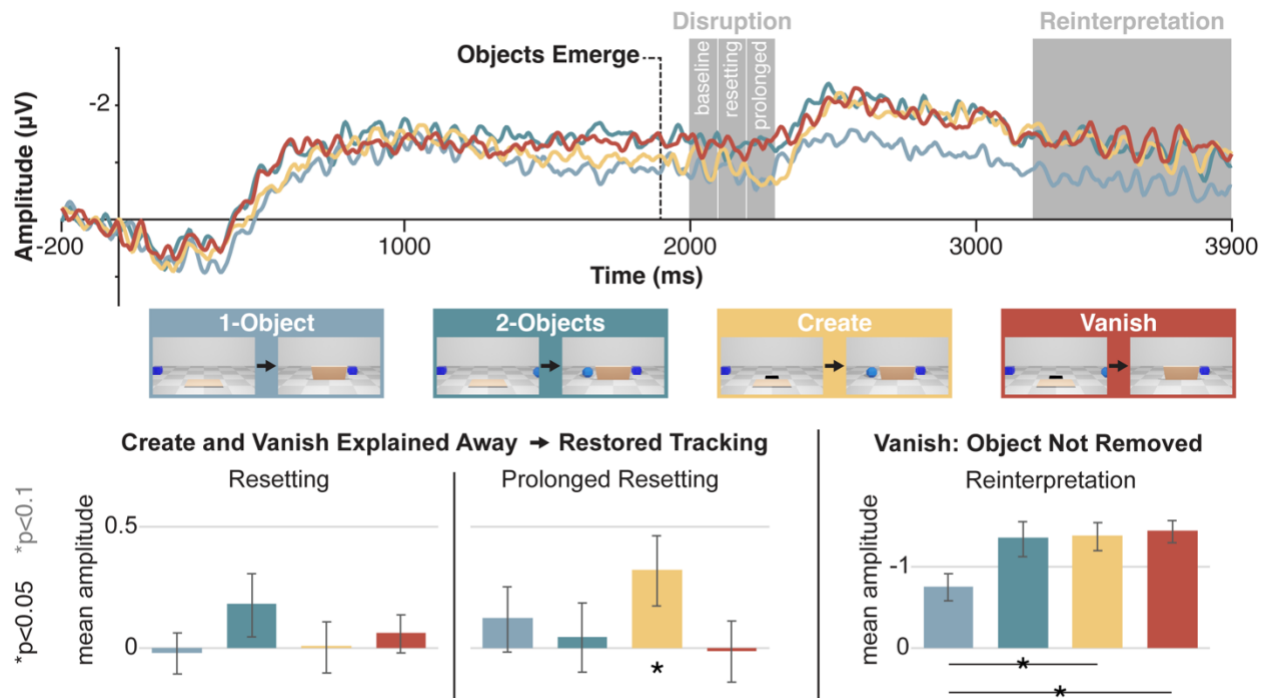
391 given the long presentation time after items exit from behind the occluder. The mean
392 accuracy in the Create condition was lower than in the 1-Object Control ($M = 0.78$ vs. 0.93 ;
393 $F(1, 15) = 100.8$, $p < 0.001$, $d = 2.5$, $95\% \text{ CI} = [0.12, 0.19]$), and similar to the mean accuracy
394 in the 2-Objects Control ($M = 0.79$; $F < 1$, $p = 0.4$, $d = 0.2$, $95\% \text{ CI} = [-0.02, 0.04]$). These
395 results match the item load at the end of the trial. The mean accuracy in the Vanish
396 condition was lower than in the 1-Object Control ($M = 0.88$; $F(1, 15) = 31.1$, $p < 0.001$, $d =$
397 1.4 , $95\% \text{ CI} = [0.03, 0.08]$), and higher than the 2-Objects Control ($F(1, 15) = 20.8$, $p < 0.001$,
398 $d = 1.1$, $95\% \text{ CI} = [0.05, 0.13]$) and Create ($F(1, 15) = 68.4$, $p < 0.001$, $d = 2.1$, $95\% \text{ CI} = [0.08,$
399 $0.13]$) conditions. So, even though the CDA amplitude indicated a successful removal of the
400 item that disappeared, its presence in the first part of the trial still produced a cost relative
401 to one object.

402

403 **Experiment 2: Online representations depend on expectations**

404 In Experiment 2, we tested whether changing the interpretation of scenes can affect the
405 moment-by-moment dynamics of object maintenance and tracking. New participants ($n =$
406 16) watched short animations that were identical to Experiment 1, except that the Create
407 and Vanish conditions included a small black rectangle behind the rising screen (Figure
408 1B), which was described to participants as a hole that objects could climb up from or fall
409 into. The hole was hidden behind the screen when objects emerged, making the scenes
410 perceptually-identical to Experiment 1 during the critical moments. The two experiments
411 diverged only in terms of participant expectations, as the appearance or disappearance of
412 items could now be explained away (Perez and Feigenson, 2022).

413 As in the previous experiment, we examined potential disruptions to the pointer
414 system by comparing the resetting time-window, and the subsequent time-window, to the
415 baseline time-window immediately before any CDA-drop, and found a significant
416 interaction of Time and Condition ($F(3,45) = 4.18, p = 0.01$). If physical expectations govern
417 online object tracking over and above low-level factors, then making the Create and Vanish
418 scenes physically possible should eliminate the resetting effect. Accordingly, as can be seen
419 in Figure 5, we found that there was no resetting effect for Create nor Vanish (both F 's < 1 ,
420 both p 's > 0.4 , both d 's < 0.2 ; Create 95% CI = [-0.22, 0.23]; Vanish 95% CI = [-0.11, 0.23]).
421 In the following time-window, there was no resetting effect for Vanish ($F < 1, p = 0.9, d = 0$,
422 95% CI = [-0.26, 0.28]), but there was one for Create ($F(1,15) = 4.59, p = 0.049, d = 0.5, 95\%$
423 CI = [0.0, 0.63]). Possibly it was more difficult to explain an appearance, and to predict
424 which exact object will emerge.



425

426 **Figure 5.** EEG results for Experiment 2. Top: CDA waveforms by condition. Dashed line
 427 indicates when objects emerge behind the lowering screen. Analyzed time-windows are in
 428 grey. Bottom: Mean amplitude by condition and time-window; error bars show standard
 429 error. From left to right: Resetting minus baseline (indicating object tracking disruption),
 430 immediately following window minus baseline (indicating prolonged object tracking
 431 disruption), and retention interval amplitude (indicating scene reinterpretation, i.e., the
 432 number of represented objects at the end of the trial). Asterisks show significant (black)
 433 and marginally significant (grey) contrasts.

434

435 We next examined whether there was a resetting effect in the Control conditions,
 436 which were identical to the Control conditions of Experiment 1. As a reminder, we found
 437 some weak evidence for this effect in the Control conditions of Experiment 1, and posited it
 438 is likely an artifact. In Experiment 2, we found no drop effect in the Control conditions, in

439 either the resetting time-window (1-Object Control: $F(1, 15) = 1.76$, $p = 0.2$, $d = 0.3$, 95% CI
440 = [-0.11, 0.45]; 2-Objects Control: $F < 1$, $p = 0.8$, $d = 0.1$, 95% CI = [-0.16, 0.2]) or the
441 prolonged resetting window (both F 's < 1 , both p 's > 0.3 , both d 's < 0.3 ; 1-Object Control
442 95% CI = [-0.17, 0.41]; 2-Objects Control 95% CI = [-0.26, 0.35]). Because the Control
443 conditions were identical in Experiment 1 and 2, the non-effect in Experiment 2 suggests
444 that indeed the marginal evidence for resetting in Experiment 1's Control conditions had
445 something to do with the context produced by the impossible conditions, in line with recent
446 work (Friedman and Luria, 2022). This further shows that the resetting results of
447 Experiment 1 do not reflect a condition-general effect (e.g., as the need to track items
448 through occlusion, or an overall reduction in CDA amplitude over time).

449 As with Experiment 1, we established how the scenes are interpreted after all the
450 events took place by comparing the final CDA amplitude across the different conditions,
451 which resulted in a significant effect of Condition ($F(3,45) = 4.46$, $p = 0.008$). We found that
452 in the Create condition, the final CDA amplitude followed the updated number of objects in
453 the scene, in that it was higher than the 1-Object Control ($F(1,15) = 11.4$, $p = 0.004$, $d = 0.8$,
454 95% CI = [0.23, 1.02]), and similar to the 2-Objects Control ($F < 1$, $p = 0.9$, $d = 0.0$, 95% CI =
455 [-0.41, 0.47]). Interestingly, in the Vanish condition the amplitude was also significantly
456 above the 1-Object Control ($F(1,15) = 11.57$, $p = 0.004$, $d = 0.9$, 95% CI = [0.26, 1.13]), and
457 similar to the 2-Objects Control ($F < 1$, $p = 0.7$, $d = 0.1$, 95% CI = [-0.4, 0.6]), as well as the
458 Create condition ($F < 1$, $p = 0.7$, $d = 0.1$, 95% CI = [-0.4, 0.6]). This result suggests that
459 participants continued to hold the vanished object in WM, even though, as in Experiment 1,
460 the object disappeared from view, and was never probed during the memory test. The item
461 that 'fell down the hole' is out of view, but still part of the scene. This suggests that online

462 representations are not determined simply by predictability (which would lead
463 participants to never represent the to-be-vanished item), but also by physical explanations.

464 Again for completeness, we examined people's behavioral performance on the
465 memory task, finding a significant effect of Condition on accuracy ($F(3,45) = 33.89, p <$
466 0.001). We found the same pattern as in Experiment 1. The mean accuracy in the Create
467 condition was lower than in the 1-Object Control ($M = 0.79$ vs. $0.93; F(1, 15) = 61.47, p <$
468 $0.001, d = 2.0, 95\% CI = [0.09, 0.16]$), and similar to the 2-Objects Control ($M = 0.8; F(1, 15)$
469 $= 1.71, p = 0.2, d = 0.3, 95\% CI = [-0.01, 0.04]$). The mean accuracy in the Vanish condition
470 was lower than in the 1-Object Control ($M = 0.88; F(1, 15) = 11.58, p = 0.004, d = 0.9, 95\%$
471 $CI = [0.02, 0.09]$), and higher than the 2-Objects Control ($F(1, 15) = 16.52, p = 0.001, d = 1.0,$
472 $95\% CI = [0.03, 0.1]$) and Create ($F(1, 15) = 21.92, p < 0.001, d = 1.2, 95\% CI = [0.05, 0.12]$)
473 conditions. So, while people's behavioral memory performance was the same across
474 Experiment 1 and 2, their online dynamics diverged. This again shows the importance of
475 tools like the CDA in uncovering hidden representational dynamics.

476

477

478

479 **Discussion**

480

481 Our findings show for the first time how violations of intuitive physics are processed
482 moment-by-moment to support object tracking and WM updating. We presented scenes
483 inspired by developmental studies and AI benchmarks in a WM task, and monitored the
484 neural dynamics of processing physically surprising events. Specifically, we examined the

485 CDA (Vogel and Machizawa, 2004; McCollough et al., 2007; Luria et al., 2016), an ERP index
486 of online processing, in two different ways. First, the presence or absence of a CDA-drop
487 after a given event indicated whether this event prevented objects in the scene to continue
488 being tracked (Balaban and Luria, 2017, 2019; Balaban et al., 2018a, 2019). Second,
489 comparing the CDA amplitude between different conditions showed how the scenes were
490 represented in WM after each event took place. The novel use of a well-established
491 electrophysiological marker revealed that violations of object permanence disrupt the
492 pointer system's ability to track objects (Experiment 1), due to expectations about physical
493 outcomes (Experiment 2).

494 The disruption of tracking during violations of physical expectations sheds light on
495 the principles governing the normal function of the pointer system. First, the presence of a
496 resetting effect in the Vanish condition shows that an event does not have to be
497 perceptually salient to disrupt object tracking. Second, the resetting effect in the Create
498 condition suggests that the pointer system is sensitive to the physical aspects of the scene
499 in tracking objects: The new object's appearance is only "impossible" in the sense that it
500 should not have appeared in a place that was previously empty (note that the mere
501 appearance of a new object in a scene does not in itself trigger resetting; (Balaban and
502 Luria, 2017). Taken together, these two effects suggest that in maintaining a continuous
503 correspondence between the perceptual input and the active representations in WM, the
504 pointer system is not solely driven by low-level factors, as is usually assumed in
505 discussions of object tracking (for a review of this subject, see Holcombe, 2023). While the
506 pointer system obviously relies on visual input, the present results show that it also
507 incorporates the physical interpretation of visual events (Lau and Brady, 2020).

508 Our findings suggest that the brain’s tracking system predicts an object’s future
509 location based on intuitive physics, perhaps via noisy quantitative physical simulation
510 (Battaglia et al., 2013; Ullman et al., 2017; Smith et al., 2019). Our results help explain
511 numerous separate past findings, which showed pointer system resetting following
512 violations of object separation (Balaban and Luria, 2017; Balaban et al., 2018a, 2018b,
513 2019a), object replacement (Balaban and Luria, 2017; Friedman and Luria, 2022), and
514 feature switching (Park et al., 2020). While these situations were not originally explained in
515 such a way, they violate cohesion, object permanence, and kind-identity, respectively.

516 The CDA further allowed us to decipher people’s flexible interpretation of events,
517 and how it changes to fit the inferred meaning of the unfolding scene. We found that WM
518 recovers after resetting within the time frame examined, and that scene representations
519 are correctly adjusted to add or remove objects (Experiment 1), based not only on what is
520 available in perception, but also on the physical explanations of events (Experiment 2).
521 This highlights another way in which common sense physical understanding shapes WM’s
522 online representations, over and above low-level visual properties.

523 The results of our experiments do not reflect surprise itself, but rather a disruption
524 of the pointer system. We found this system to be sensitive to physical violations, which
525 could feed downstream to a surprise signal. The experiments also show that the disruption
526 of the pointer system can be mitigated by expectations, but that this mitigation depends on
527 the format of the expectations. In Experiment 1, participants saw the stimuli dozens of
528 times, which forms the overall statistical expectation that in principle objects can
529 sometimes disappear or appear in the videos. This statistical expectation did not prevent a
530 robust and repeated disruption of tracking. By contrast, the expectations in Experiment 2

531 were successful in eliminating the disruption. But, these expectations had a perceptual and
532 causal format tied to a specific stimulus: the hole in the ground explained causally why on
533 this trial an object might disappear or appear, and did so in the same visual format as the
534 rest of the stimuli. Past studies of resetting in the pointer system support the distinction
535 between expectation formats: Numerous exposures to a disruptive event did not eliminate
536 the disruption, and even making a disruptive event perfectly predictable failed to do so
537 (Balaban et al., 2019b), but subtle visual cues that altered the way the scene was carved
538 into distinct objects, thereby changing the targets for tracking, were successful right away
539 (e.g., Balaban et al., 2019a). Future work can adopt the present approach to further
540 examine how the pointer system communicates with other processes, by looking at what
541 other physical situations and expectations disrupt or preserve object tracking, including
542 perceptually weak but causally specific expectations such as telling participants the rising
543 screen acts as a magic box on specific trials. While more work is needed, our conclusion is
544 not just that the pointer system's ability to track objects is based on physical reasoning, but
545 that the format of this physical reasoning matters.

546 Our findings introduce a novel way of tackling both new and outstanding open
547 questions. Identifying different cognitive processes from task performance measures alone
548 (e.g., accuracy or reaction time) can be challenging, as they may reflect the sum of all
549 processing stages. While behavioral performance is useful and important, apparent task
550 effects in online processing tasks might not reflect WM or object tracking, but sub-stages
551 that precede or follow them, such as perception or decision making (Awh et al., 2007). This
552 may be why measures of performance on WM or tracking tasks can show mixed results
553 with regards to intuitive physics (e.g., vanMarle and Scholl, 2003; Mitroff et al., 2004;

554 Franconeri et al., 2012). In contrast, the CDA factors out contributions of perceptual facets
555 (Ikkai et al., 2010; Luria et al., 2010; Ye et al., 2014), by using a bilateral paradigm. It also
556 factors out response-related facets, by focusing the analysis on the period preceding the
557 test phase, meaning before participants can initiate any response. The step-by-step neural
558 analysis of online processing, tracking, and representations allows researchers to address
559 the different sub-stages of intuitive physics that underlie overt surprise, and can tease
560 apart generic surprise from the violation of intuitive physics more specifically. A
561 developmentally appropriate version of measuring a CDA-like pattern in infants can also
562 potentially establish that infant overt surprise in the face of physically impossible events
563 reflects disrupted physics-based object tracking. This can be expanded to other cases that
564 robustly show behavioral surprise based on violations of expectations. In the physical
565 domain, some events are surprising without interfering with tracking, such as a mug falling
566 off a table and bouncing, which could reveal that it is made out of rubber, which is
567 physically surprising but does not interfere with tracking. In the psychological domain,
568 both adults and young children are surprised when agents act in an inefficient way (e.g.,
569 Baillargeon et al., 2016). Nevertheless, we would predict such surprise would not lead to
570 resetting, as this violation does not interfere with object tracking.

571 More generally, our method can shed light on how people perceive, track,
572 understand, and remember physical events, by bridging traditional cognitive science,
573 developmental psychology, and neuroscience perspectives. We see great promise in hybrid
574 approaches that, as we do here, use simplified but ecologically foundational stimuli based
575 on infant studies, while measuring well-characterized neural markers resting on years of
576 rigorous quantitative validation from carefully controlled psychological experiments with

577 adults. Examining the CDA in this novel manner allowed us to reveal previously-hidden
578 influences of intuitive physics on everyday representation, understanding, and reasoning.

579 **References**

580

581 Awh E, Barton B, Vogel EK (2007) Visual Working Memory Represents a Fixed Number of
582 Items Regardless of Complexity. *Psychol Sci* 18:622–628.

583 Baddeley A (1992) Working Memory. *Science* 255:556–559.

584 Baillargeon R, Scott RM, Bian L (2016) Psychological Reasoning in Infancy. *Annu Rev*
585 *Psychol* 67:159–186.

586 Baillargeon R, Spelke ES, Wasserman S (1985) Object permanence in five-month-old
587 infants. *Cognition* 20:191–208.

588 Balaban H, Drew T, Luria R (2018a) Delineating resetting and updating in visual working
589 memory based on the object-to-representation correspondence. *Neuropsychologia*
590 113:85–94.

591 Balaban H, Drew T, Luria R (2018b) Visual working memory can selectively reset a subset
592 of its representations. *Psychon Bull Rev* 25:1877–1883.

593 Balaban H, Drew T, Luria R (2019a) Neural evidence for an object-based pointer system
594 underlying working memory. *Cortex* 119:362–372.

595 Balaban H, Drew T, Luria R (2019b) Neural evidence for a dissociation between the pointer
596 system and the representations of visual working memory. *Journal of Vision* 19:82c.

597 Balaban H, Luria R (2015) The number of objects determines visual working memory
598 capacity allocation for complex items. *NeuroImage* 119:54–62.

599 Balaban H, Luria R (2016a) Integration of Distinct Objects in Visual Working Memory
600 Depends on Strong Objecthood Cues Even for Different-Dimension Conjunctions.
601 Cereb Cortex 26:2093–2104.

602 Balaban H, Luria R (2016b) Object representations in visual working memory change
603 according to the task context. Cortex 81:1–13.

604 Balaban H, Luria R (2017) Neural and Behavioral Evidence for an Online Resetting Process
605 in Visual Working Memory. J Neurosci 37:1225–1239.

606 Balaban H, Luria R (2019) Using the Contralateral Delay Activity to Study Online Processing
607 of Items Still Within View. In: Spatial Learning and Attention Guidance (Pollmann S,
608 ed), pp 107–128 Neuromethods. New York, NY: Springer US.

609 Battaglia PW, Hamrick JB, Tenenbaum JB (2013) Simulation as an engine of physical scene
610 understanding. Proc Natl Acad Sci USA 110:18327–18332.

611 Bear DM, Wang E, Mrowca D, Binder FJ, Tung H-YF, Pramod RT, Holdaway C, Tao S, Smith K,
612 Sun F-Y, Fei-Fei L, Kanwisher N, Tenenbaum JB, Yamins DLK, Fan JE (2021) Physion:
613 Evaluating Physical Prediction from Vision in Humans and Machines. Available at:
614 <https://arxiv.org/abs/2106.08261>.

615 Blaser E, Pylyshyn ZW, Holcombe AO (2000) Tracking an object through feature space.
616 Nature 408:196–199.

617 Cacchione T, Krist H (2004) Recognizing Impossible Object Relations: Intuitions About
618 Support in Chimpanzees (*Pan troglodytes*). *Journal of Comparative Psychology*
619 118:140–148.

620 Carlisle NB, Arita JT, Pardo D, Woodman GF (2011) Attentional Templates in Visual
621 Working Memory. *J Neurosci* 31:9315–9322.

622 Delorme A, Makeig S (2004) EEGLAB: an open source toolbox for analysis of single-trial
623 EEG dynamics including independent component analysis. *Journal of Neuroscience*
624 *Methods* 134:9–21.

625 Drew T, Horowitz TS, Vogel EK (2013) Swapping or dropping? Electrophysiological
626 measures of difficulty during multiple object tracking. *Cognition* 126:213–223.

627 Drew T, Horowitz TS, Wolfe JM, Vogel EK (2012) Neural Measures of Dynamic Changes in
628 Attentive Tracking Load. *Journal of Cognitive Neuroscience* 24:440–450.

629 Drew T, Vogel EK (2008) Neural Measures of Individual Differences in Selecting and
630 Tracking Multiple Moving Objects. *J Neurosci* 28:4183–4191.

631 Feldmann-Wüstefeld T, Vogel EK, Awh E (2018) Contralateral Delay Activity Indexes
632 Working Memory Storage, Not the Current Focus of Spatial Attention. *Journal of*
633 *Cognitive Neuroscience* 30:1185–1196.

634 Fischer J, Mikhael JG, Tenenbaum JB, Kanwisher N (2016) Functional neuroanatomy of
635 intuitive physical inference. *Proc Natl Acad Sci USA* 113.

636 Franconeri SL, Pylyshyn ZW, Scholl BJ (2012) A simple proximity heuristic allows tracking
637 of multiple objects through occlusion. *Atten Percept Psychophys* 74:691–702.

638 Friedman S, Luria R (2022) Visual working memory adaptability: What more can we learn
639 about updating and resetting of visual working memory representations? *Journal of*
640 *Vision* 22:3465–3465.

641 Holcombe A (2023) *Attending to Moving Objects*, 1st ed. Cambridge University Press.

642 Ikkai A, McCollough AW, Vogel EK (2010) Contralateral Delay Activity Provides a Neural
643 Measure of the Number of Representations in Visual Working Memory. *Journal of*
644 *Neurophysiology* 103:1963–1968.

645 Kahneman D, Treisman A, Gibbs BJ (1992) The reviewing of object files: Object-specific
646 integration of information. *Cognitive Psychology* 24:175–219.

647 Kang M-S, Woodman GF (2014) The neurophysiological index of visual working memory
648 maintenance is not due to load dependent eye movements. *Neuropsychologia*
649 56:63–72.

650 Kubricht JR, Holyoak KJ, Lu H (2017) *Intuitive Physics: Current Research and*
651 *Controversies*. *Trends in Cognitive Sciences* 21:749–759.

652 Lau JS-H, Brady TF (2020) Noisy perceptual expectations: Multiple object tracking benefits
653 when objects obey features of realistic physics. *Journal of Experimental Psychology:*
654 *Human Perception and Performance* 46:1280–1300.

655 Lopez-Calderon J, Luck SJ (2014) ERPLAB: an open-source toolbox for the analysis of event-
656 related potentials. *Frontiers in Human Neuroscience* 8.

657 Luck SJ, Vogel EK (1997) The capacity of visual working memory for features and
658 conjunctions. *Nature* 390:279–281.

659 Luria R, Balaban H, Awh E, Vogel EK (2016) The contralateral delay activity as a neural
660 measure of visual working memory. *Neuroscience & Biobehavioral Reviews* 62:100–
661 108.

662 Luria R, Sessa P, Gotler A, Jolicœur P, Dell’Acqua R (2010) Visual Short-term Memory
663 Capacity for Simple and Complex Objects. *Journal of Cognitive Neuroscience*
664 22:496–512.

665 Luria R, Vogel EK (2011a) Visual Search Demands Dictate Reliance on Working Memory
666 Storage. *Journal of Neuroscience* 31:6199–6207.

667 Luria R, Vogel EK (2011b) Shape and color conjunction stimuli are represented as bound
668 objects in visual working memory. *Neuropsychologia* 49:1632–1639.

669 McCollough AW, Machizawa MG, Vogel EK (2007) Electrophysiological Measures of
670 Maintaining Representations in Visual Working Memory. *Cortex* 43:77–94.

671 Mitroff SR, Scholl BJ, Wynn K (2004) Divide and conquer: How object files adapt when a
672 persisting object splits into two. *Psychological Science* 15:420–425.

673 Park B, Walther D, Fukuda K (2020) Dynamic Representations in Visual Working
674 Memory. *Journal of Vision* 20:900.

675 Perez J, Feigenson L (2022) Violations of expectation trigger infants to search for
676 explanations. *Cognition* 218:104942.

677 Peterson DJ, Gözenman F, Arciniega H, Berryhill ME (2015) Contralateral delay activity
678 tracks the influence of Gestalt grouping principles on active visual working memory
679 representations. *Atten Percept Psychophys* 77:2270–2283.

680 Piloto LS, Weinstein A, Battaglia P, Botvinick M (2022) Intuitive physics learning in a deep-
681 learning model inspired by developmental psychology. *Nat Hum Behav* 6:1257–
682 1267.

683 Pylyshyn ZW (2000) Situating vision in the world. *Trends in Cognitive Sciences* 4:197–207.

684 Scholl BJ, Pylyshyn ZW (1999) Tracking Multiple Items Through Occlusion: Clues to Visual
685 Objecthood. *Cognitive Psychology* 38:259–290.

686 Smith K, Mei L, Yao S, Wu J, Spelke E, Tenenbaum J, Ullman T (2019) Modeling Expectation
687 Violation in Intuitive Physics with Coarse Probabilistic Object Representations. In:
688 *Advances in Neural Information Processing Systems*. Curran Associates, Inc.

689 Spelke ES (1990) Principles of object perception. *Cognitive Science* 14:29–56.

690 Tsubomi H, Fukuda K, Watanabe K, Vogel EK (2013) Neural Limits to Representing Objects
691 Still within View. *J Neurosci* 33:8257–8263.

692 Ullman TD, Spelke E, Battaglia P, Tenenbaum JB (2017) Mind Games: Game Engines as an
693 Architecture for Intuitive Physics. *Trends in Cognitive Sciences* 21:649–665.

- 694 vanMarle K, Scholl BJ (2003) Attentive Tracking of Objects Versus Substances. *Psychol Sci*
695 14:498–504.
- 696 Vogel EK, Machizawa MG (2004) Neural activity predicts individual differences in visual
697 working memory capacity. *Nature* 428:748–751.
- 698 Vogel EK, McCollough AW, Machizawa MG (2005) Neural measures reveal individual
699 differences in controlling access to working memory. *Nature* 438:500–503.
- 700 Wynn K (1992) Addition and subtraction by human infants. *Nature* 358:749–750.
- 701 Xu F, Carey S (1996) Infants' Metaphysics: The Case of Numerical Identity. *Cognitive*
702 *Psychology* 30:111–153.
- 703 Ye C, Zhang L, Liu T, Li H, Liu Q (2014) Visual Working Memory Capacity for Color Is
704 Independent of Representation Resolution Martinez LM, ed. *PLoS ONE* 9:e91681.